Slow-Motional NMR Line Shapes for Very Anisotropic Rotational Diffusion. Phosphorus-31 NMR of Phospholipids

R. F. Campbell,† E. Meirovitch,‡ and J. H. Freed*

Department of Chemistry, Cornell University, Ithaca, New York 14853 *(Received August 21, 1978)*

The model of Mason, Polnaszek, and Freed for ESR-slow-tumbling spectra is extended to the case of NMR line shapes for arbitrary tilt of the internal axis of relatively rapid rotation with respect to the principal axes of the chemical shielding tensor for a decoupled $I = 1/2$ nucleus. The theory is applied to an analysis of ^{31}P NMR spectra from partially hydrated dipalmitoylphosphatidylcholine (DPPC) molecules over a range of temperature. Generally, very good agreement with experiment is obtained enabling the determination of the rate of the "average" or "effective" internal rotation and the orientation of this "average" axis in the molecule. The basis on which the simple model reflects the spectral effects of the combined internal and overall motions is discussed in detail in an appendix, and the extension to more complex models is outlined.

(I) Introduction

The model of very anisotropic rotational reorientation in slow-motional spectra was treated several years ago by Mason et al.[1] for the case where a nitroxide electron spin probe is undergoing relatively rapid rotation about a single bond, while the macromolecule to which it is attached is reorienting slowly. In the present study we extend this type of approach to cover nuclear spin probes ($I = 1/2$ nuclei) and we treat the more general case of a primary axis for diffusion which is tilted at arbitrary angle from the principal axes of rotational diffusion. The specific manner in which this model effectively includes internal modes of motion is also considered here in somewhat greater detail. The method is suited for the analysis of internal motions in macromolecules with the option of choosing a probe nucleus, e.g., ^{1}H, ^{31}P, ^{19}F, ^{13}C, ^{15}N, etc. (occurring either naturally or by means of specific isotope labeling), depending on the nature of the molecule investigated and the time scale of the dynamical processes taking place.

To illustrate the method we have chosen ^{31}P NMR spectra from the DPPC molecule which consists mainly of a glycerol residue to which are attached two long fatty acid chains and the phosphatidylcholine head group. This phospholipid molecule is of particular interest, since phospholipid bilayers are a major component of biological membranes. The importance of the head-group structure of the phospholipid molecule is today well established; that is, one observes a variation of phospholipid head-group composition in different systems[2] and also one finds specific phospholipid requirements of various membranal enzymes.[3] There seems to be a direct relationship between the type of the head group present and the fluidity of the phospholipid dispersions; the gel to liquid crystalline thermal phase transition temperature is sensitive to the nature of the head group as well as to the presence of head-group perturbations such as Ca^{2+} and pH; the cooperativity of the various phase transitions in phospholipid bilayers is related to the head-group structure[4] and the biaxial nature of low water content phospholipid bilayers is also related to the head-group conformation.[5-7]

Fully hydrated bilayers of DPPC have been thoroughly studied by a variety of methods, in order to determine the bilayer structure and the molecular conformations of the DPPC molecule, with a particular emphasis on the geometry as well as the dynamic characteristics of the head-group region. However, in view of the great geometric and dynamic complexity of these systems, the experimental data could not be interpreted unambiguously, and several models consistent with the various experimental findings have been suggested.[8-12]

Lower water content mixtures have recently been investigated by various methods.[13-15] ^{31}P NMR experiments[15] have shown that upon complete dehydration, the rigid-limit powder spectrum is obtained, and the spectral changes upon increasing the water content have been interpreted in terms of the onset of head-group motion, which leads to motionally averaged spectra at 15 °C for ca. 15%, by weight, water. Below the gel to liquid crystalline phase transition (occurring at 41 °C for fully hydrated DPPC bilayers and at somewhat higher temperatures for lower water content[6]) the long fatty acid residues are found to be crystalline-like. When the water content is lowered, the complexity of the dynamic processes is substantially decreased, and the dominant process is the reorientation of the head group.[15] We show, in this work, how we are able to characterize this process in terms of anisotropic diffusion coefficients at the various temperatures as well as the orientation of the principal diffusion axis in the molecular frame, by means of a complete line-shape analysis of ^{31}P NMR spectra from the rigid limit up to the limit of rapid anisotropic rotational reorientation.

In section II we develop the theoretical method for the basic model of slow tumbling and very anisotropic diffusion and then give typical results to illustrate the slow-tumbling range and to determine the limiting conditions under which the simpler approaches used previously are valid. In section III we analyze the experimental results for a mixture of DPPC and 15%, by weight, water in terms of the theoretical simulations and we discuss their implications. The limitations of the present analysis are pointed out there as well as the potential for further studies. Experimental details appear in section IV. The more general theoretical discussion of the combined slow-tumbling spectral effects of both overall reorientation and internal rotations and the relationship of more general models to our model of section II appears in Appendix A.

(II) Theory

(A) *Spin Hamiltonian* [^{31}P]. The spin Hamiltonian appropriate for NMR, written in the spherical tensor convention of Freed and Fraenkel,[16] is

$$\mathcal{H}(\Omega) = \sum_{\substack{L=0,2 \\ K,M,\mu,i}} (-1)^K \mathcal{D}^L_{K,M}(\Omega) F^{(L,K)}_{\mu,i} A^{(L,M)}_{\mu,i} \qquad (1)$$

† NIH Postdoctoral Fellow.
‡ Chaim Weizmann Postdoctoral Fellow.

0022-3654/79/2083-0525$01.00/0

where the $F^{\langle L,K\rangle}_{\mu,i}$ and $A^{(L,M)}_{\mu,i}$ represent the irreducible tensor components of rank L and components K and M, respectively, with μ distinguishing the different types of magnetic interactions and i, the different magnetic nuclei. The $F^{\langle L,K\rangle}_{\mu,i}$ are functions of the magnetic parameters of the system expressed in the molecule-fixed, diffusion axis system, while the $A^{(L,M)}_{\mu,i}$ are functions only of the spin operators quantized in the laboratory axis system. The $\mathcal{D}^{(L)}_{-K,M}(\Omega)$ are Wigner rotation matrix elements which express the transformation from the molecule-fixed (x', y', z') to the laboratory (x, y, z) axis system, where Ω represents the Euler angles (α, β, γ) relating one axis system to the other.

When the principal axis systems of the magnetic interaction (x''', y''', z''') and those of the molecule-fixed, diffusion (x', y', z') are noncoincident an additional transformation with Euler angles $\Psi = (\psi, \theta, \varphi)$ must be made between these axis systems. This is given by

$$F^{\langle L,K\rangle}_{\mu,i} = \sum_{K'} \mathcal{D}^{(L)}_{K,K'}(\Psi) F'''^{\langle L,K'\rangle}_{\mu,i} \tag{2}$$

where, for the case of axially symmetric rotational diffusion, Ψ reduces to $(0, \theta, \varphi)$ where θ and φ represent the polar angles of this axis in the (x''', y''', z''') coordinates.

For an $I = 1/2$ system, such as phosphorus-31, where the internuclear dipolar interaction may be neglected in the presence of a strong, externally applied decoupling field, the spin Hamiltonian reduces to just the effect of the chemical shielding tensor, so that

$$\mathcal{H}(\Omega) = -\gamma_N(1 - \sigma)B_0 I_z + \sqrt{\frac{2}{3}}\gamma_N B_0 I_z \sum_{m=-2 \text{ to } +2} (-1)^m \mathcal{D}^{(2)}_{-m,0}(\Omega) F^{\langle 2,m\rangle}_{cs} \tag{3}$$

Explicitly, the $F^{\langle 2,m\rangle}_{cs}$ components for $\Psi = (0, \theta, \varphi)$ are

$$F^{\langle 2,0\rangle}_{cs} = \left[\frac{1}{2}(3\cos^2\theta - 1)\right] F'''^{\langle 2,0\rangle}_{cs} + \left[\sqrt{\frac{3}{2}}\cos 2\varphi \sin^2\theta\right] F'''^{\langle 2,\pm 2\rangle}_{cs} \tag{4a}$$

$$F^{\langle 2,1\rangle}_{cs} = \left[-\sqrt{\frac{3}{2}}\sin\theta\cos\theta\right] F'''^{\langle 2,0\rangle}_{cs} + [\cos 2\varphi \sin\theta\cos\theta - i \sin 2\varphi \sin\theta] F'''^{\langle 2,\pm 2\rangle}_{cs} = -F^{\langle 2,-1\rangle *}_{cs} \tag{4b}$$

$$F^{\langle 2,2\rangle}_{cs} = \left[\sqrt{\frac{3}{8}}\sin^2\theta\right] F'''^{\langle 2,0\rangle}_{cs} + \left[\cos 2\varphi\left(\cos^4\left(\frac{\theta}{2}\right) + \sin^4\left(\frac{\theta}{2}\right)\right) - i \sin 2\varphi\left(\cos^4\left(\frac{\theta}{2}\right) - \sin^4\left(\frac{\theta}{2}\right)\right)\right] F'''^{\langle 2,\pm 2\rangle}_{cs} = F^{\langle 2,-2\rangle *}_{cs} \tag{4c}$$

and the $F'''^{\langle 2,m\rangle}_{cs}$ are given in Table I. We have dropped the nonsecular ($I_\pm$) terms in eq 3, because in high magnetic fields they make a negligible contribution to the (slow-tumbling) spectrum.[1] [Furthermore, we may note that in high magnetic fields, when nonsecular terms are negligible, we can treat nuclei with quadrupole moments, e.g., ^{2}H or ^{14}N, by nearly identical methods applied to each of the allowed transitions, and similar comments apply to the case of dipolar interactions between like spins of $I = 1/2$.]

(B) *Rotational Model.* Now, in general, the Euler angles $\Omega = (\alpha, \beta, \gamma)$ are fluctuating due to the overall reorientational motion as well as due to the various internal rotations which can affect the subgroup containing the magnetic nucleus. This is expected to be true for phospholipid head-group motion which probably involves multiple rotation axes. Mason et al.[1] pointed out that rather than consider a very complex analysis of such motions and their spectral effects, it is useful in most cases to simplify the model to include two primary rotational diffusion coefficients in a manner that is formally equivalent to axially symmetric rotational diffusion wherein $R_\parallel$ (the parallel component of the rotational diffusion tensor) represents the relatively rapid internal rotational motion (or the net effect of several such motions) while $R_\perp$ represents the net effect of the slow overall motions. This was indeed found to be an adequate model for initial analyses given the limited but useful "information content" of the "slow-tumbling" spectra. (In fact Mason et al.[1] only considered the case of $\varphi = 0$ in order to reduce the more complex analysis required for nitroxide spin probes to a reasonably tractable level.)

TABLE I

		chemical shielding interaction	
		$l = 0$	$l = 2$
$A^{(l,q)}_{\mu,I}$	$q = 0$	$B_0 I_z$	$(2/3)^{1/2} B_0 I_z$
	$q = \pm 1$	0	$\pm B_0 I_\pm$
	$q = \pm 2$	0	0
$F'''^{(l,m)}_{\mu}$	$m = 0$	$^1/_3$ Tr $(\sigma - 1)^a$	$(3/2)^{1/2}(\sigma_{z'''z'''} - {}^1/_3 \text{ Tr } \sigma)$
	$m = \pm 1$	0	0
	$m = \pm 2$	0	$^1/_2(\sigma_{x'''x'''} - \sigma_{y'''y'''})$

[a] $^1/_3$ Tr $\sigma \equiv \sigma_0$.

For our analysis, we employ this simplified model of Mason et al., except that the "full-tilt" case of $\theta \neq 0$ and $\varphi \neq 0$ is employed, since the spin Hamiltonian of eq 3 and 4 is simpler, so the overall slow-tumbling problem is more tractable. We show in Appendix A how more complex and realistic models involving relatively rapid internal rotation and overall slower reorientation do indeed reduce to the *form* of our simple approach under several physically realistic limiting cases. For each of these cases one obtains more precise interpretations of the phenomenological $R_\parallel$ and $R_\perp$, the interpretation of the tilt angles, and the conditions under which the more general treatment outlined in Appendix A might be required. Thus, for example, it is possible to show that for a molecule undergoing completely anisotropic rotational diffusion (with principal components $R_{x'}$, $R_{y'}$, and $R_{z'}$) and with relatively much more rapid internal rotation of the subgroup containing the magnetic nucleus (with internal rotational coefficient R_I) that $R_\parallel$ can indeed be interpreted as R_I, while the complex overall motion may be represented by a single "effective" R (or $R_\perp$) which is a weighted average of $R_{x'}$, $R_{y'}$, and $R_{z'}$ that depends upon the orientation of the axis of internal rotation relative to the principal axes (x', y', z') of the overall rotational diffusion tensor. (This is case 5 in Appendix A.) It is also pointed out how the method may be extended to multiple internal rotations.

Thus we continue the analysis below as though we are dealing with simple axially symmetric rotational diffusion, but when we come to interpret the ^{31}P NMR spectra, we make use of the interpretation that appears appropriate based upon the discussion in Appendix A.

(C) *Stochastic Liouville Expressions.* Here we follow the usual approach of FBP[17-20] in evaluating the stochastic Liouville equation (SLE) for this case of a single $I = 1/2$ nuclear spin. [This is formally analogous to the ESR problem of a single spin of $S = 1/2$ with an asymmetric **g** tensor, given by FBP, but we now allow for arbitrary orientation of the main diffusion axis with respect to the principal axes of the magnetic tensor.] One obtains the

following compact set of coupled algebraic equations for the coefficients C^L_{KM} in the eigenfunction expansion of the density matrix (cf. Appendix A and ref 17–20), which determines the slow-tumbling spectrum:

$$[(\omega - \omega_0) - i(T_2^{-1} + \tau_{L,K}^{-1})]\bar{C}^{L\pm}_{K,0} + (-1)^{K+1}F^{\langle 2,0\rangle}\sum_{L'}\hat{N}_K(L,L',0)\bar{C}^{L'\pm}_{K,0} + (-1)^K\sum_{L'}\hat{N}_K(L,L',-1)[(\pm 1)\ \mathrm{Im}\ F^{\langle 2,1\rangle})\bar{C}^{L'\mp}_{K+1,0} + (\mathrm{Re}\ F^{\langle 2,1\rangle})\bar{C}^{L'\pm}_{K+1,0}] + (-1)^K\sum_{L'}\hat{N}_K(L,L',+1)[(\pm 1)\times (\mathrm{Im}\ F^{\langle 2,1\rangle})\bar{C}^{L'\mp}_{K-1,0} - (\mathrm{Re}\ F^{\langle 2,1\rangle})\bar{C}^{L'\pm}_{K-1,0}] + (-1)^{K+1}\sum_{L'}\hat{N}_K(L,L',-2)[(\mathrm{Re}\ F^{\langle 2,2\rangle})\bar{C}^{L'\pm}_{K+2,0} + (\pm 1)(\mathrm{Im}\ F^{\langle 2,2\rangle})\bar{C}^{L'\mp}_{K+2,0}] + (-1)^{K+1}\sum_{L'}\hat{N}_K(L,L',2)[(\mathrm{Re}\ F^{\langle 2,2\rangle})\bar{C}^{L'\pm}_{K-2,0} - (\pm 1)\times (\mathrm{Im}\ F^{\langle 2,2\rangle})\bar{C}^{L'\mp}_{K-2,0}] = \sqrt{2}\delta(L,0)\delta(K,0) \quad (5)$$

where we have used the definitions

$$\bar{C}^{L+}_{K,0} \equiv \frac{1}{\sqrt{2}}[C^L_{K,0} + (-1)^K C^L_{-K,0}] \qquad K > 0 \qquad (6a)$$

$$\bar{C}^{L-}_{K,0} \equiv \frac{i}{\sqrt{2}}[C^L_{K,0} - (-1)^K C^L_{-K,0}] \qquad K > 0 \qquad (6b)$$

$$\bar{C}^{L+}_{0,0} \equiv \sqrt{2}C^L_{0,0} \qquad (6c)$$

while $\bar{C}^{L-}_{0,0}$ is nonexistent. Also

$$\hat{N}_K(L,L',K') \equiv N(L,L')\begin{pmatrix} L & 2 & L' \\ -K & K' & K-K' \end{pmatrix}\begin{pmatrix} L & 2 & L' \\ 0 & 0 & 0 \end{pmatrix} \quad (7)$$

in terms of the $3-j$ symbols, and $N(L,L') \equiv [(2L+1)(2L'+1)]^{1/2}$. Also, ω is the frequency of the resonant rf field, while $\omega_0 = \gamma_N(1-\sigma)B_0$; T_2^{-1} is an orientation-independent residual line width; the $\tau_{L,K}^{-1}$ are the eigenvalues of the diffusion operator for axially symmetric diffusion in an isotropic medium, and for Brownian rotational diffusion they are given by

$$\tau_{L,K}^{-1} = [R_\perp L(L+1) + (R_\parallel - R_\perp)K^2] \qquad (8)$$

where $R_\perp$ and $R_\parallel$ are respectively the perpendicular and parallel components of the diffusion tensor. The $\tau_{L,K}^{-1}$ for other models of rotational reorientation are given elsewhere.[18-20] Note that (Re $F^{\langle 2,P\rangle}$) and (Im $F^{\langle 2,P\rangle}$) are the real and imaginary parts of $F^{\langle 2,P\rangle}$, respectively, which may be obtained from eq 4a.

Note that the absorption spectrum $I(\omega - \omega_0)$ is given by

$$I(\omega - \omega_0) \propto \mathrm{Im}\ C^0_{0,0} \qquad (9)$$

The infinite set of equations given by eq 5 may be written in matrix notation as

$$\mathbf{AC} = \mathbf{U} \qquad (10)$$

where $\mathbf{C}$ is a column vector of all the coefficients, $\bar{C}^{L\pm}_{KM}$, while $\mathbf{A}$ is seen from eq 5 to be a complex-symmetric matrix, which can be rewritten as $\mathbf{A} = \mathbf{A}' + K\mathbf{1}$ with $K = \omega - \omega_0 - iT_2^{-1}$ so that $\mathbf{A}'$ does not contain the sweep variable. Equations 5 (or 10) and 9 were solved in the standard manner[18-20] by first diagonalizing $\mathbf{A}'$. The computer program, written for an IBM 370/168 computer, allows for K truncation.[19,20] Typical values for L and K which are required for $R_\parallel >> R_\perp$ with the latter being very slow were $L = 20$ and $K = 2$, with computing times of 10 CPU s. [This program also allows for a cylindrically-symmetric orienting potential $U(\Omega)/kT = -\lambda\cos^2\beta$, such that the primary axis of the molecular diffusion tensor tends to be ordered with respect to the applied dc magnetic field. The methods for including orienting potentials have been given elsewhere.[19-22]] Copies of this program are available from the authors.

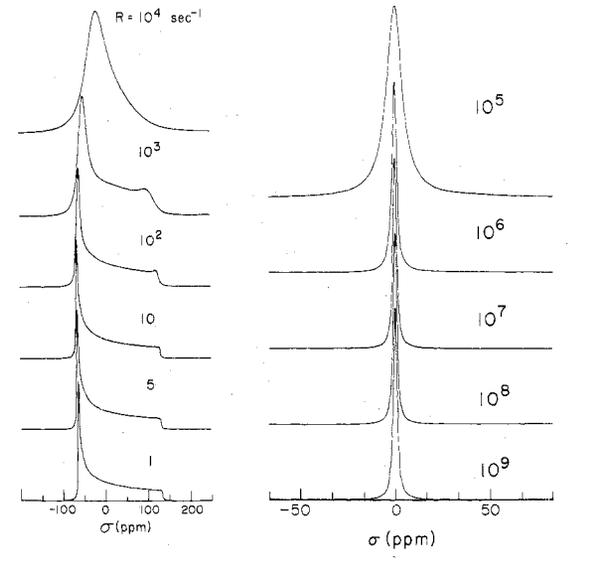

Figure 1. Theoretical spectra illustrating the changes in the line shape occurring as a function of R, the rate of isotropic Brownian diffusion, as denoted in the figure (in units of s^{-1}), for an axially symmetric tensor with $\sigma_\parallel = -65$ ppm, $\sigma_\perp = 130$ ppm, and a residual line width $T_2^{-1} = 1$ ppm. The calculations were performed using L values as large as 90 for the near-rigid-limit region ($R = 5$–$1\ s^{-1}$), $L = 8$ for the slow-motional region ($R \simeq 10^4\ s^{-1}$), and $L = 4$ for the limit of rapid motion ($R = 10^5$–$10^9\ s^{-1}$).

(D) *Spectral Simulations.* (1) *Range of Slow-Motional Spectra.* The sensitivity of a typical NMR spectrum for a spin $I = 1/2$ with an anisotropic chemical shift to rates of molecular motion from 1 to $10^9\ s^{-1}$ is illustrated in Figure 1. For simplicity, we have chosen an axially symmetric σ tensor with $\sigma_\parallel = -65$ ppm and $\sigma_\perp = 130$ ppm and an isotropic Brownian rotational diffusion process with a rate $R = 1/(6\tau_R)$, with τ_R denoting the correlation time for rotational diffusion. The overall width of the rigid-limit spectrum is 300 ppm and the residual line width is 1 ppm. This would correspond to nuclei such as ^{31}P, ^{13}C, and ^{19}F which have chemical shift anisotropies of several hundred ppm and to spectrometers equipped with high decoupling power units (to decouple abundant surrounding nuclei from the observed nucleus) so as to obtain a small residual line width. It was shown recently[23] that for a macroscopically isotropic hydrated DPPC sample the residual line width is less than 1 ppm both for ^{13}P and for ^{13}C, using a spectrometer suited for solid-state NMR. The slow-motional region includes the range $10 \lesssim R \lesssim 10^5$ and is sensitive to the details of molecular dynamics.

To illustrate the sensitivity of the line shape to the orientation of the axis about which axially symmetric rotational diffusion occurs, we have chosen typical values of $R_\parallel = 1.58 \times 10^4\ s^{-1}$ and $R_\perp = 1.58 \times 10^2\ s^{-1}$ ($\tau_R = 1.05 \times 10^{-4}$ s), where $\tau_R = 1/(6(R_\parallel R_\perp)^{1/2})$ and $T_2^{-1} = 10$ ppm representing anisotropic slow tumbling, but we varied the polar angles θ and φ which define the orientation of the diffusion axis relative to the coordinate system determined by the principal axes of the ^{31}P chemical shift tensor, as shown in Figure 2.

For simplicity, we have ignored the possibility of a microscopic ordering potential at the position of the ^{31}P nucleus; the excellent fit between the experimental and simulated spectra (Figure 5) is certainly consistent with this assumption although there is a more fundamental justification given below. However, there is experimental

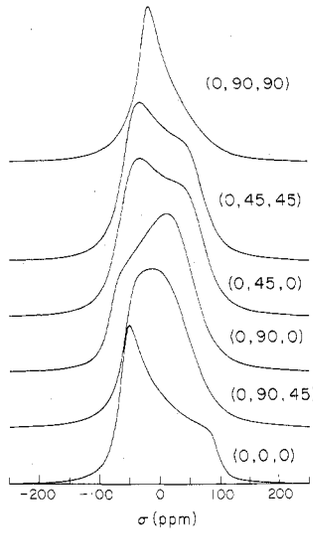

Figure 2. Theoretical spectra illustrating the changes in the line shape occurring upon varying the polar angles θ and φ as denoted in the figure. The simulations were performed with $R_{\parallel} = 1.58 \times 10^4$ s^{-1}, $R_{\perp} = 1.58 \times 10^2$ s^{-1}, $T_2^{-1} = 10$ ppm, and $L = K = 14$.

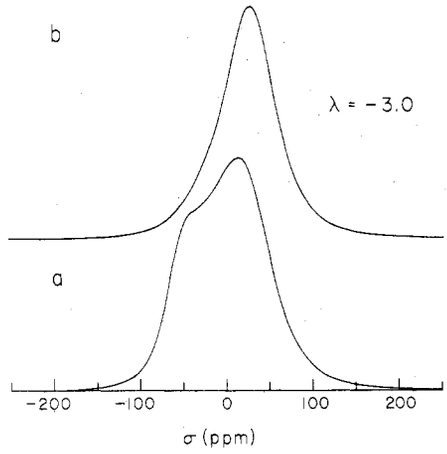

Figure 3. Theoretical spectra illustrating the effect on the line shape of including in the calculation an ordering potential. The simulations were performed for $\tau_R = 3.33 \times 10^{-5}$ s, $T_2^{-1} = 5$ ppm, $R_{\parallel}/R_{\perp} = 10$, $\theta = 90°$, $\varphi = 0°$, $L = 10$, and $K = 10$. In trace (a) no ordering potential was used and in trace (b) an axially symmetric orienting potential $U(\beta)/kT = -\lambda \cos^2 \beta$ with λ -3.0 was used.

evidence[24] that microscopic ordering indeed occurs in the case of fully hydrated (40% H_2O) DPPC bilayers. To illustrate the effect of a macroscopic ordering potential, we present in Figure 3(a) the line shape for $R_{\parallel}/R_{\perp} = 10$, $\tau_R = 3.33 \times 10^{-5}$ s, $T_2^{-1} = 5$ ppm, $\theta = 90°$, and $\varphi = 0°$, to be compared with the line shape in Figure 3(b), where a simple axially symmetric potential with $\lambda = -3.0$ has been included. As seen, the dominant effect is to transform the line-shape features to a near rapid motional spectrum. We emphasize this point to show that the theory may be used to treat cases of nonzero ordering potentials which are certainly relevant for oriented phospholipid bilayers. In the special limiting case of microscopic order but macroscopic disorder (e.g., polycrystalline samples) where motion relative to the microscopic ordering forces has reached the rigid limit (but any other motions such as internal rotation could still be evident in the spectrum), one immediately concludes that the spectrum is correctly predicted without having to include the microscopic ordering in the analysis. This will be seen to be the correct limit for the analysis of the ^{31}P spectra in Figure 5.

(2) *Validity of Simple Limiting Cases.* Many workers[8-12] have used a simple limiting model of very rapid

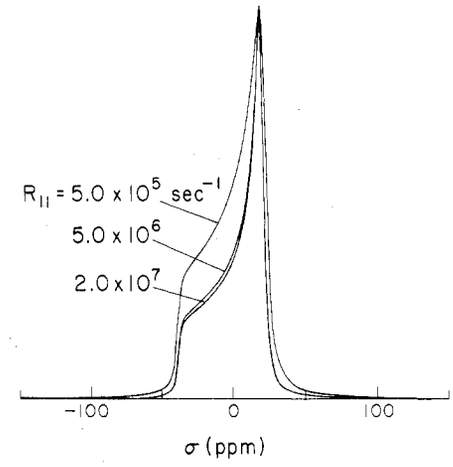

Figure 4. Theoretical spectra to determine the lower limit of $R_{\parallel}$ for which the assumption of rapid very anisotropic motion is rigorously valid. The values $R_{\perp} = 5$ s^{-1}, $\theta = 87.8°$, $\varphi = 69°$, $T_2^{-1} = 1.6$ ppm, $L = 32$, and $K = 2$ were used. The spectra also illustrate the small effect of decreasing $R_{\parallel}$ from its limiting value of ca. 2×10^7 s^{-1} on the "apparent" $\Delta\sigma = \tilde{\sigma}_{\parallel} - \tilde{\sigma}_{\perp}$ which is directly measured from the spectrum.

anisotropic reorientation. In this section we consider its range of validity. Rapid very anisotropic motion implies that the rotational dynamics of the spin about some molecular diffusion axis v is very fast, while motion perpendicular to that axis is very slow. Such an approximation is only rigorously correct where (1) the motion about v, which is described by an effective rotational diffusion tensor component $R_{\parallel}$, is so fast that residual time-dependent effects of the averaging process, which lead to line broadening, etc. are negligible and (2) the motion perpendicular to v, described by an effective $R_{\perp}$ is so slow that its effects on the spectrum are negligible. We show in Figure 4 simulated ^{31}P spectra which allow one to determine the values of $R_{\parallel}$ and $R_{\perp}$ for which the above criteria are achieved.

We found that these limiting values are $R_{\parallel} \geq 2 \times 10^7$ s^{-1} and $R_{\perp} \leq 5$ s^{-1} for the particular values of the shielding tensor, θ, φ, and T_2^{-1} corresponding to our experimental spectra presented in the following section.

Further, we found that the anisotropy of the axially symmetric line shape, defined by[9] $\Delta\tilde{\sigma} \equiv \tilde{\sigma}_{\parallel} - \tilde{\sigma}_{\perp}$, where $\tilde{\sigma}_{\parallel}$ and $\tilde{\sigma}_{\perp}$ denote the positions of the extremes in the line shape, is not significantly affected when the above criterion for $R_{\parallel}$ is not fully achieved. For example, one finds from Figure 4 that even though $R_{\parallel}$ is as much as 2 orders of magnitude smaller than that required to meet the above rigorous criterion, the main effect is that of line broadening, whereas the positions of the extremes $\tilde{\sigma}_{\parallel}$ and $\tilde{\sigma}_{\perp}$ are not significantly different from their value for rapid very anisotropic motion. However, an accurate determination of $\Delta\sigma$, without a complete line-shape analysis, is certainly made difficult by the line broadening.

We point out that previous approaches for analyzing ^{31}P line shapes[9,11] were based upon determining $\Delta\sigma$ from the extremes in the absorption pattern assuming rapid very anisotropic reorientation (i.e., very fast $R_{\parallel}$ and very slow $R_{\perp}$) as well as ignoring the possibility of microscopic ordering. Implications regarding the orientation of the diffusion axis as well as a lower limit for $R_{\parallel}$[9] were derived, using the expression

$$\Delta\tilde{\sigma} = \tfrac{1}{2}(3\cos^2\theta - 1)[\sigma_{zz} - \tfrac{1}{2}(\sigma_{xx} + \sigma_{yy})] + \tfrac{3}{4}(\sigma_{xx} - \sigma_{yy})\sin^2\theta\cos 2\varphi \quad (11)$$

which is rigorously valid only if all the assumptions listed above are fulfilled. We have shown in our above discussion that even though approximate values for θ,φ sets which

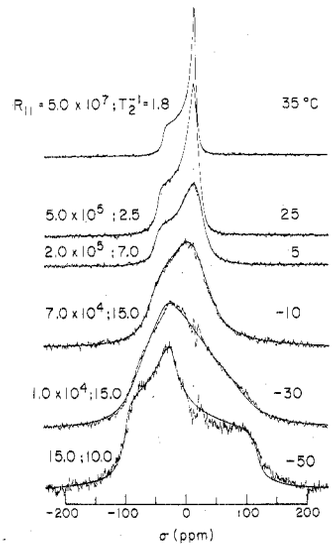

Figure 5. Experimental ^{31}P NMR spectra recorded using a WH 270 Brucker spectrometer equipped with a superconducting magnet: dwell time 10 μs, repetition time 2 s, pulse length 8 μs. Quadrature detection was used and about 200 free induction decays were accumulated for the higher temperature spectra and about 2000 for the lower temperature spectra. The broad-band ^{1}H decoupling power was 15 W. The smooth lines are theoretical simulations with $\sigma_x = -100$, $\sigma_y = -30$, and $\sigma_z = -130$ ppm, $R_\perp = 5$ s^{-1}, and $\theta = 87.8°$; the value of φ was 55° for the -30 to -5° C simulations, 58° for the 25 °C simulation and 69° for the 35 °C simulation; the residual line width T_2^{-1} in ppm and the values for R in s^{-1} are denoted in the figure. The simulations were performed using $L = 32$ and $K = 2$ for the theoretical spectra corresponding to 35 and 25 °C, $L = 20$ and $K = 2$ for the 5 °C simulation, $L = 20$ and $K = 4$ for the -10 and -30 °C simulations, and $L = 40$ for the -50 °C simulation. The rigid-limit spectrum was simulated with a computer program generating a powder pattern corresponding to a chemical shift tensor with $\sigma_x = -100$, $\sigma_y = -30$, and $\sigma_z = 130$ ppm, $T_2^{-1} = 10$ ppm and a Lorentzian line shape; the fit of this spectrum with the -50 °C experimental trace was found to be very good.

fulfill eq 11 can be obtained, it is still possible that $R_{\|}$ is as much as 2 orders of magnitude smaller than the lower limit upon which the simple model is based. Thus one should be very careful in using that approach.

We now comment on the likely possibility that a slow-motional spectrum might be analyzed as if it were a rigid-limit pattern. One should note in Figure 1 that the very slow motional spectra exhibit shapes similar to that of the rigid limit but $\Delta\tilde{\sigma}$ is smaller. Thus, in one analysis of DPPC monohydrate spectrum as a rigid-limit pattern,[9] values for the components of the chemical shift tensor were obtained, which are smaller than the dehydrated powder.[15] It might well be that slow-motional effects are responsible for this discrepancy, so one should always consider this possibility and record rigid-limit spectra at lower temperatures until no further spectral changes are observed.

(III) Experimental Results for ^{31}P and Their Analysis

The experimental ^{31}P spectra are presented in Figure 5 together with the theoretical spectra obtained as described in section II. In the following, we (a) discuss the physical model to be associated with the theoretical simulations, (b) explain the approach taken in simulating the experimental spectra, and (c) conclude with general results of the analysis as well as implications of the data regarding head-group conformation and dynamics at the upper temperature regions studied.

The physical model is based on that of simple axially symmetric rotational diffusion of the ^{31}P moiety about an internal rotation axis defined in the head group which could be arbitrarily tilted with respect to the principal axes of the chemical shielding tensor. Further, we assumed the following:

(1) The orientation of the principal axes of the ^{31}P chemical shift tensor in the DPPC molecule is identical with that determined for the PO_4 group by Griffin et al.[13]

(2) The principal values of the chemical shift tensor remain unchanged throughout the temperature range examined.

(3) An upper limit to the value of $R_\perp$, which can be determined from the rapid anisotropically averaged DPPC spectrum at 35 °C, may be used for all other temperatures studies (i.e., only the values of $R_{\|}$, θ, and φ are affected by changes in temperature).

(4) For the set of experimental spectra from -50 to +25 °C, the orientation of the principal axes for rotational diffusion with respect to those of the chemical shielding tensor remains essentially fixed.

On the basis of these assumptions, we could interpret in an internally consistent manner the changes in the line shape occurring upon varying the temperature between -100 and +55 °C, in terms of rotational diffusion rates and orientation of an "averaged" or "effective" diffusion axis. In the analysis, the input parameters are T_2^{-1}, $R_{\|}$, $R_\perp$, θ, and φ, as well as the σ tensor. The value of $R_\perp$ used was $R_\perp \leq 5$ s^{-1} and was found to be determined by simulation of the rapid motionally averaged +35 °C spectrum. For the low-temperature spectra T_2^{-1} is of the order of 10 ppm, based on the simulation of the rigid-limit pattern obtained at -50 °C.

For the high-temperature spectra T_2^{-1} was found to be of the order of 1 ppm (Griffin et al.[21] showed that for fully hydrated DPPC at room temperature, the residual line width is about 1 ppm).

We first simulated the spectrum obtained at -50 °C, which remained unchanged upon lowering the temperature to -100 °C. Taking this to be the rigid-limit pattern, we obtained, via a best fit simulation, $\sigma_x = -100$ ppm, $\sigma_y = -30$ ppm, $\sigma_z = 130$ ppm, and $T_2^{-1} = 10$ ppm. We then proceeded by simulating the experimental spectrum at 35 °C (which does not change upon increasing the temperature to 55 °C), by varying $R_{\|}$, $R_\perp$, T_2^{-1}, θ, and φ. After determining $\Delta\tilde{\sigma}$ and using eq 11 and the best fit values of θ and φ, we then calculated sets of θ and φ satisfying this equation: we obtained θ within the range $60° < \theta < 90°$ and φ within the range $0 < \varphi < 65°$, defining a solid angle for the diffusion axis. The line shape could be simulated using any of these sets θ and φ with $R_{\|} \gtrsim 2 \times 10^7$ s^{-1} and $R_\perp \lesssim 5.0$ s^{-1}. (At 35 °C the values of $R_{\|}$ and $R_\perp$ could be determined, since they were found to represent the respective limiting values for rapid anisotropic reorientation.) Thus although the order of magnitude of the dynamic rates $R_{\|}$ and $R_\perp$ can be determined, the orientation of the diffusion axis cannot be determined unambiguously from the 35 °C spectrum.

According to assumption (3) we let $R_\perp \leq 5.0$ s^{-1} for the 25 °C spectrum as well as for all other temperatures below 35 °C. We obtained $R_{\|} = 5 \times 10^5$ s^{-1}. Even though $R_{\|} = 5 \times 10^5$ s^{-1} is below the limiting value of $R_{\|}$ for rapid anisotropic motion, as shown in section IID2, the parameter $\Delta\tilde{\sigma}$ is essentially unchanged. Thus, taking the same approach as with the 35 °C spectrum, we again found several sets of θ and φ, all of which gave the same simulated line shape.

The experimental series of spectra show that between 25 and 35 °C the line shape changes abruptly, whereas from -50 to 25 °C the changes in the line shape are gradual. We therefore assume that for the set of spectra from -50 to +25 °C that the orientation of the rotational diffusion

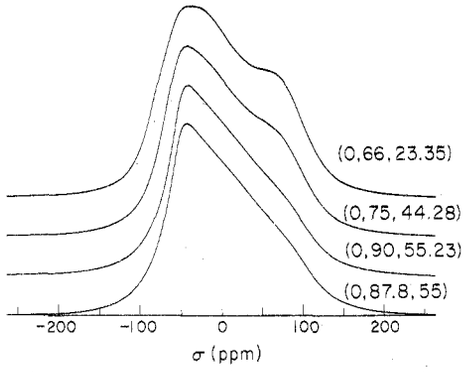

Figure 6. Theoretical spectra illustrating the sensitivity of slow-motional spectra (corresponding to the experimental spectrum recorded at −30 °C) to the values of θ and φ, for $R_{\parallel} = 1.0 \times 10^4$ s^{-1}, $R_{\perp} = 5$ s^{-1}, and $T_2^{-1} = 10$ ppm. The calculations were performed using $L = 20$ and $K = 4$.

frame remains essentially fixed. Thus, we proceeded by choosing one of the sets θ,φ obtained as described above for 25 °C and simulated the spectra recorded at 5, −10, and −30 °C by only decreasing the values of $R_{\parallel}$ and allowing for a increase in the intrinsic line width with decreasing temperature. (The intrinsic line width is due to the residual dipolar couplings between the ^{31}P nucleus and the surrounding ^{1}H nuclei; similar to the dynamic averaging out of the ^{31}P chemical shift anisotropy, these dipolar interactions are also gradually averaged out as the rate of the head-group motion increases.) In contrast to the results for the higher temperature spectra, Figure 6 shows that simulations of the −30 °C spectrum (reflecting slow reorientation) are sensitive to the set of θ and φ chosen. This result is not surprising, since it was shown in previous ESR studies that the slow-motional region is quite sensitive to the details of the motional dynamics. Using the result, we were then able to uniquely determine the set of θ and φ appropriate not only for the −30 °C spectrum but for the entire spectral series from +25 to −50 °C as well. The best overall fit between the experimental and the simulated spectra was obtained for $\theta = 88°$ and $\varphi = 55°$, as shown in Figure 5 and it is seen to be very good in all cases. The diffusion axis does not coincide with any of the chemical bonds in the vicinity of the ^{31}P atom (based on the identity of the various bond angles in DPPC and in the phosphodiester barium diethylphosphate model compound[13]) and this is probably indicative of an "average" or "effective" diffusion axis over the entire head group, represented schematically in Figure 7. We obtain an activation energy for the process (cf. Figure 5) of 10.3 ± 0.5 kcal/mol.

The sudden change in the line shape at 35 °C indicates both a considerable change in the value of $R_{\parallel}$ and a variation in the orientation of the diffusion axis from $\theta = 88°$ and $\varphi = 58°$ at 25 °C to any of the sets θ and φ which fulfill eq 11 for which $\theta = 88°$ and $\varphi = 69°$ is representative (see upper trace in Figure 5). Although the exact nature of this transition is not known, our experiments imply a change of head-group conformation. Since 34 °C is the temperature at which the pretransition has been observed in fully hydrated (>40% H_2O) DPPC, it is reasonable to relate this phenomenon to our observation.

Further NMR studies using, for example, ^{13}C-labeled DPPC may be of great value in trying to clarify the situation at 35 °C. Given the additional information regarding θ and φ provided by the ^{13}C spectra, one will most probably be able to obtain a unique determination of the orientation of the diffusion axis at 35 °C.

We conclude with the following:

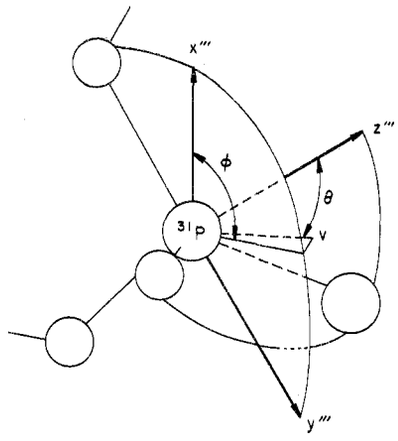

Figure 7. Schematic representation of the PO_4 group in the DPPC molecule; x''', y''', and z''' denote the principal axes of the chemical shift tensor of the ^{31}P nucleus based on ref 9, and θ and φ define the orientation of the diffusion axis v for the process occurring between −50 and +25 °C, relative to this coordinate system; axis y''' lies within the O–P–O plane and approximately bisects the O–P–O angle, where the O's are the nonesterified oxygens.

(1) The ^{31}P line shape is sensitive to the rate of anisotropic rotation over 5–6 orders of magnitude.

(2) The changes in the line shape with temperature are generally interpretable in terms of a simple model of anisotropic rotation about a unique "effective" diffusion axis, allowing the determination of both the rate of rotational dynamics and the direction of the diffusion axis between −50 and +25 °C.

(3) There is an apparent change in head-group conformation between 35 and 25 °C as evidenced by both a considerable change in the value of $R_{\parallel}$ as well as a change in the orientation of the diffusion axis.

(4) The method used is potentially suited to deal with several coupled motions (cf. Appendix A). As expected, the slow-motional spectra are sensitive to the motional details. The full power of the method in elucidating details of complex dynamic processes can be exercised using several probes in the same molecule, e.g., ^{31}P, ^{15}N, ^{13}C, ^{1}H, ^{19}F, etc. nuclei with different principal axes of the chemical shift tensors (or else with different ratios of the components with the same principal axes). The present study will be further pursued along this line.

Such an approach will hopefully enable one to understand more complex systems, such as fully hydrated DPPC bilayers, leading to an unambiguous description of microscopic structure and dynamics.

(IV) Experimental Section

Homogeneous mixtures of DPPC powder (purchased from Sigma) and distilled deionized water were obtained by adding the appropriate amount of water, 15% by weight, to the phospholipid and mixing thoroughly. The purity of DPPC was checked by standard methods: thin-layer chromatography and gel to liquid crystalline phase transition temperature of a dispersion of DPPC in excess water.

The FT NMR ^{31}P spectra were recorded on a WH 270 Brucker spectrometer equipped with a superconducting magnet. The following settings were used for all spectra: pulse width 8 μs, dwell time 10 μs, repetition time 2 s, broad-band ^{1}H decoupling power 15 W. The number of free induction decays accumulated were about 200 for the high-temperature spectra and 2000 for the low-temperature spectra, and quadrature detection was used.

Temperature control was achieved using a stream of heated or cooled nitrogen at the sample. The probe temperature was measured in a separate experiment using a phospholipid sample with an imbedded thermocouple, and the spectrometer was adjusted to the same experiment settings as those used during the main experiment. The estimated stability in the temperature is ±1 °C above room temperature and ±2 °C below room temperature. Since it was shown[15] that the ^{31}P spectra are sensitive to the water content, the reversibility of the spectra on cooling or heating was used as a check on the constancy of the water content and, in general, as a check that no irreversible changes occurred during the experiment.

Acknowledgment. This work was supported by NSF Grants CHE77-26996 and DMR 77-17510. We gratefully acknowledge the use of the WH 270 NMR spectrometer of the Isotope Department of the Weizmann Institute of Science, Rehovot, Israel.

Appendix A. General Considerations for Models Involving Relatively Rapid Internal Rotation

We show in this appendix how the simple model of section II based on axially symmetric rotational diffusion may be applied and extended to situations involving internal rotations. We start with eq 1, but we now generalize eq 2 to

$$F^{(L,K)}_{\mu,i} = \sum_{K',K''} \mathcal{D}^{L}_{KK'}(\Theta)\mathcal{D}^{L}_{K'K''}(\Psi)F'''^{(L,K'')}_{\mu,i} \qquad \text{(A1)}$$

where Ψ represents the Euler angles for the transformation between the principal axes of magnetic interaction (x''', y''', z''') located in an internal rotor of the molecule (e.g., the PO_4 group) and a principal axis system (x^{iv}, y^{iv}, z^{iv}) fixed in the main frame of the molecule, such that the Euler angles Ψ include the angle of internal rotational motion. Then the Euler angles Θ represent the transformation between the molecular axes (x^{iv}, y^{iv}, z^{iv}) and the principal axes of rotational diffusion (x', y', z').

More precisely, we consider the axis of internal rotation as the z^{iv} axis, and its orientation is specified by the polar angles θ and φ in the magnetic tensor (x''', y''', z''') coordinate system. Then, if we let ψ represent the angle of rotation about the axis of internal rotation, we have $\Psi = (\psi, \theta, \varphi)$. Furthermore, if we assume axially symmetric rotational diffusion of the backbone or main portion of the molecule, then we can let $\Theta = (0, \beta', \gamma')$, where β' and γ' are the polar angles of this principal axis of diffusion referred to the (x^{iv}, y^{iv}, z^{iv}) system. Note that we may then write[25] $\mathcal{D}^{L}_{K'K''}(\Psi) = e^{iK'\psi}\,\mathcal{D}^{L}_{K'K''}(0, \theta, \psi)$ where only $e^{iK'\psi}$ is fluctuating in time (as a result of the internal motion).

Now, in the solution of the SLE we expand the orientation-dependent spin-density matrix $\sigma(\Omega)$ in eigenfunctions of the diffusion operator,[12-22] which is in the present case just $\Gamma_\Omega + \Gamma_\psi$ if we neglect for simplicity any coupling between the internal rotational motion (with diffusion operator Γ_ψ) and the overall rotational motion (with diffusion operator Γ_Ω) and treat them as independent processes. We can use the $\varphi^{L}_{KM}(\Omega) = N_L{}^{1/2}\mathcal{D}^{L}_{KM}(\Omega)$ with $N_L = (2L + 1)/(8\pi^2)$ as the normalized eigenfunctions of Γ_Ω with eigenvalues $R_\perp L^2 + (R_\parallel - R_\perp)K^2$ (since we will assume axially symmetric rotational diffusion for simplicity in presentation). The eigenfunctions for the internal rotation may be taken as the functions $(1/(2\pi)^{1/2})e^{iK'\psi}$ with eigenvalues of Γ_I (assuming simple Brownian motion) given by $R_I K'^2$, where R_I is the diffusion coefficient for this motion.[26] These results may readily be generalized to the case of jump diffusion, but the eigenfunctions will remain the same, while the eigenvalues will change somewhat.[27,28]

Thus we shall use the expansion

$$\sigma_\lambda(\Omega) = \sum_{L,K,K',M} C^{L}_{K,K',M}\varphi^{L}_{KM}(\Omega)\frac{1}{\sqrt{2\pi}}e^{iK'\psi} \equiv \sum_{L,K,K',M} C^{L}_{K,K',M}|L,K,K',M\rangle \qquad \text{(A2)}$$

for the off-diagonal matrix element of $\sigma(\Omega)$ between states $M_I = 1/2$ and $-1/2$ (represented by subscript λ). We now note that the matrix elements needed for the SLE are

$$\langle L_1K_1K_1',M_1|\Gamma_\Omega + \Gamma_I|L_2K_2K_2',M_2\rangle = [R_\perp L_1(L_1 + 1) + K_1{}^2(R_\parallel - R_\perp) + K_1'^2R_I]\delta_{L_1,L_2}\delta_{K_1,K_2}\delta_{K_1',K_2'}\delta_{M_1,M_2} \qquad \text{(A3)}$$

and

$$\langle L_1K_1K_1',M_1|\mathcal{H}_1(\Omega,\Psi,\Theta)|L_2K_2K_2',M_2\rangle = \sum_{\substack{K,M,K_1'\\K'',\mu,i}} (-1)^K\delta_{K',K_1'-K_2'}\langle L_1K_1M_1|\mathcal{D}^{2}_{-KM}(\Omega)|L_2K_2M_2\rangle \times \mathcal{D}^{L}_{KK'}(0,\beta',\gamma')\mathcal{D}^{L}_{K'K''}(0,\theta,\varphi)F'''^{(L,K'')}_{\mu,i}A^{(L,M)}_{\mu,i} \qquad \text{(A4)}$$

where we have used eq 1 and A1 to express $\mathcal{H}_1(\Omega_1,\Psi,\Theta)$.[29]

Thus our model, and the associated NMR spectrum in the (slow) motional region are completely determined by the diffusion coefficients $R_\parallel$, $R_\perp$, and R_I and by the two pairs of polar angles β',δ' and θ, φ, for a total of seven parameters. [It is assumed that the $F'''^{(L,K'')}_{\mu,i}$ have previously been determined from rigid-limit spectra.] These represent too many variables to be confidently fit by fairly simple NMR spectra. For this reason, and also in order to reduce the complexity of the computer program, we consider some simpler limiting cases of the general model.

Case 1: Let $R_\parallel \sim R_\perp \sim R$, i.e., Spherically Symmetric Overall Diffusion. In this case we can let $\beta' = \gamma' = 0$, since there is no preferred axis of overall rotational diffusion. Then, we can write

$$\mathcal{H}_1(\Omega,\Psi) = \sum_{\substack{K,K',K''\\M,\mu,i}} (-1)^M\mathcal{D}^{2}_{-MK}(-\alpha,-\beta,-\gamma)\delta_{KK'}e^{iK'\psi} \times \mathcal{D}^{2}_{K',K''}(0,\theta,\varphi)F'''^{(L,K'')}_{\mu,i}A^{(L,M)}_{\mu,i} = \sum_{\substack{K,K''\\M,\mu,i}} (-1)^M\mathcal{D}^{2}_{-MK} \times (-\gamma,-\beta,-\alpha+\psi)\mathcal{D}^{2}_{KK''}(0,\theta,\varphi)F'''^{(L,K'')}_{\mu,i}A^{(L,M)}_{\mu,i} \qquad \text{(A5)}$$

[where we have used the fact that $\mathcal{D}^{L}_{-KM}(\alpha,\beta,\gamma) = (-)^{K+M}\mathcal{D}^{L}_{MK}(-\alpha,-\beta,-\gamma)$ in the first equality of eq A5]. It follows from the form of eq A5 that it is now sufficient to expand $\sigma_\lambda(\Omega)$ in the $\varphi^{L}_{KM}(\alpha-\psi,\beta,\gamma) = N_L{}^{1/2}\mathcal{D}^{L}_{KM}(\alpha-\psi,\beta,\gamma)$ basis set [since only the L, K, and M "quantum numbers" appear in terms in $\mathcal{H}_1(\Omega,\Psi)$ that are affected by the motions]. Then, in this basis set we get the matrix elements

$$\langle L_1K_1M_1|\Gamma_\Omega + \Gamma_\Psi|L_2K_2M_2\rangle = [RL_1(L_1 + 1) + R_IK^2]\delta_{L_1,L_2}\delta_{K_1,K_2}\delta_{M_1,M_2} \qquad \text{(A6)}$$

and for the matrix elements of $\mathcal{H}_1(\Omega_1,\Psi)$ we need

$$\langle L_1K_1M_1|\mathcal{D}^{2}_{KM}(\alpha-\psi,\beta,\gamma)|L_2K_2M_2\rangle = \frac{1}{2\pi}\langle e^{-iK_1\psi}|e^{iK\psi}|e^{iK_2\psi}\rangle\langle L_1K_1M_1|\mathcal{D}^{2}_{KM}(\alpha,\beta,\gamma)|L_2K_2M_2\rangle = \delta_{K,K_1-K_2}\delta_{M,M_1-M_2}\langle L_1K_1M_1|d^{2}_{KM}(\beta)|L_2K_2M_2\rangle \qquad \text{(A7)}$$

where the reduced Wigner rotation elements $d^{L}_{KM}(\beta)$ are defined in the usual manner.[25] We note that this last result is independent of whether we consider the matrix element involving ψ.

This case is then seen to be formally equivalent to the result for simple axially symmetric rotational diffusion wherein $R_\perp$ is replaced by R and $(R_\parallel - R_\perp)K^2$ is replaced by R_IK^2, and where the original Euler angle α is replaced by $\alpha - \psi$, while the angles β' and γ are replaced by θ and

φ, respectively. Thus, the computer program based on the analysis of section II may be used for this model.

Case 2: The Axis of Internal Rotation is Coincident with the z' Symmetry Axis for the Overall Rotational Diffusion. Then we again have $\beta' = \gamma' = 0$, so $\mathcal{D}^L_{KK'}(0,\beta',\gamma') = \delta_{K,K'}$. Again, we need only expand in the $\varphi^L_{KM}(\alpha-\psi,\beta,\gamma)$. We again obtain eq A7 but eq A6 becomes

$$\langle L_1K_1M_1|\Gamma_\Omega + \Gamma_\Psi|L_2K_2M_2\rangle = [R_\perp L_1(L_1+1) + K^2(R_I + R_\parallel - R_\perp)]\delta_{L_1,L_2}\delta_{K_1,K_2}\delta_{M_1,M_2} \quad \text{(A8)}$$

[Note that eq A8 becomes equivalent to eq A6 in the limit that $R_I >> R_\parallel, R_\perp$ if we let $R_\perp \rightarrow R$.] Thus for this case we may also use the computer program based on the analysis of section II; we need only let $R_\parallel$ in that program be redefined as $R_I + R_\parallel$, while $\alpha \rightarrow \alpha - \psi$, $\beta' \rightarrow \theta$, and $\gamma' \rightarrow \varphi$.

Case 3: Very Fast Internal Rotations. Here we assume the spectral effects of the internal motion are completely averaged out. Then, in our eigenfunction expansions we need only consider the $K_1' = 0$ or $|L_1K_10M_1\rangle$ basis set, since $\Gamma_I e^{iK'\psi} = R_I K'^2 e^{iK'\psi}$ for $K' \neq 0$ yields eigenvalues $R_\perp K'^2$ which are so much larger than any other frequencies in the problem. We then obtain the result from eq A4 of

$$\langle L_1K_1M,0|\mathcal{H}_1(\Omega_1,\Psi_1,\Theta)|L_2,K_2M_10\rangle = \sum_{\substack{K,K'',M\\ \mu,i}} (-1)^K \delta_{K',0}\langle L_1K_1M_1|\mathcal{D}^2_{-KM}(\alpha,\beta,\gamma)|L_2K_2M\rangle \times \mathcal{D}^L_{K0}(0,\beta',\gamma')\mathcal{D}^L_{0K''}(0,\theta,\varphi)F'''^{(L_2K'')}_{\mu,i}A^{(L_2M)}_{\mu,i} \quad \text{(A9)}$$

It follows from eq A9 that we can reformulate this model in terms of a redefined

$$\tilde{\mathcal{H}}_1(\Omega,\Psi_1,\Theta) \equiv \sum_{K,M,\mu,i} (-1)^K \mathcal{D}^2_{-KM}(\alpha,\beta,\gamma)\tilde{F}^{(L_2K)}_{\mu,i}A^{(L_2M)}_{\mu,i} \quad \text{(A10a)}$$

where

$$\tilde{F}^{(L_2K)}_{\mu,i} \equiv \mathcal{D}^L_{K0}(0,\beta',\gamma') \sum_{K''} \mathcal{D}^L_{0K''}(0,\theta,\varphi)F'''^{(L_2K'')}_{\mu,i} \quad \text{(A10b)}$$

and simple axially symmetric rotational diffusion for which

$$\Gamma_\Omega \mathcal{D}^L_{KM}(\Omega) = [R_\perp L_1(L_1+1) + K^2(R_\parallel - R_\perp)]\mathcal{D}^L_{KM}(\Omega) \quad \text{(A11)}$$

The $\tilde{F}^{(L_2K)}_{\mu,i}$ play the role of "apparent" tensor components of $F_{\mu,i}$ expressed in the principal axes for the overall diffusion (x', y', z') when averaged over the very rapid internal rotational motion, but we are still allowing for (a) tilting of the axis of internal rotation relative to the principal axes of the magnetic tensor given by polar angles θ and φ and (b) an angle of tilt β between the principal axis of diffusion and the axis of internal rotation. [Note that in eq A10b or A9 we can let $\mathcal{D}^L_{K0}(0,\beta',\gamma') = d^L_{K0}(\beta')$,[25] so the angle γ' is not important in this case.]

This approach for case 3 can easily be extended to handle very fast internal rotations about several bonds. It is only necessary to obtain the redefined $\tilde{F}^{(L_2K)}_{\mu,i}$ when averaged over these several motions (cf. ref 29). Then the computer program based on the analysis in section II may be used.

Case 4: Axis of Internal Rotation Coincident with Principal Axis of Magnetic Tensor, z'''. In this case $\theta = \varphi = 0$ and $\mathcal{D}^L_{K'K''}(0,\theta,\varphi) = \delta_{K',K''}$ in eq A4. This simplifies the analysis, but as long as β' and γ' are nonzero and/or $R_\parallel \neq R_\perp$, or the internal rotation is not extremely fast, then it is still necessary to expand in the $\varphi^L_{KM}(\Omega)(1/(2\pi)^{1/2})e^{iK'\psi}$ basis set (but see case 5). Thus this is a case that is still too complicated to be handled by the computer program based upon the analysis of section II, and it would require a more general program.

Case 5: General Case of Internal Rotation Being Much More Rapid Than the Overall (Anisotropic) Reorientation. We now consider the case which allows for completely anisotropic overall rotational diffusion with tensor components $R_{x'}$, $R_{y'}$, and $R_{z'}$ (in the x', y', z' coordinates) but for the limit $R_I >> R_{x'}, R_{y'}, R_{z'}$. This requires a more complex analysis than the previous cases. (Note that cases 2 and 3 are simple limits of case 5). We take as the primary set of axes of diffusion for the combined overall and internal diffusion the molecular axes (x^{iv}, y^{iv}, z^{iv}) with z^{iv} being the axis of internal rotation since the internal rotation is the fastest. The rotational diffusion tensor will not, in general, be diagonal in this coordinate frame. Thus we may write

$$\Gamma_\Omega = \boldsymbol{MRM} = \sum_{\substack{L=0,2,\\ \text{and } P}} (-1)^P \mathbf{R}^{(L,P)}(\boldsymbol{M}^2)^{(L,-P)} \quad \text{(A12)}$$

where the first equality gives the rotational diffusion operator as the dyadic scalar product involving the operator for infinitesimal rotations, $\boldsymbol{M}$ as well as the rotational diffusion tensor $\boldsymbol{R}$.[19,22,25,26,30] In the second equality it is written as a scalar product in irreducible tensor notation; the $\mathbf{R}^{(L,P)}$ and $(\boldsymbol{M}^2)^{(L,-P)}$ are formed in the usual manner[25] and are given elsewhere.[31] Similarly we may write[26]

$$\Gamma_\psi = R_I\partial^2/\partial\psi^2 \equiv R_I\boldsymbol{M}_z{}^2\psi$$

which is to be compared with $\boldsymbol{M}_{z^{iv}}{}^2 = \partial^2/\partial\alpha^2$ which appears in the $(\boldsymbol{M}^2)^{(L,-P)}$.

Note that here we may use the $\mathcal{D}^L_{KK'}(\Theta)$ (or the inverse transformation, see below) to transform the diffusion operator instead of its use in eq A1 to transform the $F^{(L_2K)}_{\mu,i}$, but, since the diffusion is not necessarily axially symmetric, we must let $\Theta = (\alpha', \beta', \gamma')$, i.e., $\alpha' \neq 0$. Thus $\mathcal{H}_1(\Omega)$ is now given by eq 1 but with eq A1 replaced by

$$F^{(L_2K)}_{\mu,i} = \sum_{K'} \mathcal{D}^L_{KK'}(\Psi)F'''^{(L_2K')}_{\mu,i} \quad \text{(A13)}$$

and the Euler angles Ω now involve the transformation between molecular (x^{iv}, y^{iv}, z^{iv}) coordinates (still defined in the molecular "backbone" system) and the lab coordinates (x, y, z). But this is seen to be analogous to the $\mathcal{H}_1(\Omega)$ for case 2, so that we see we can write $\mathcal{H}_1(\Omega,\psi)$ as eq A5 with the definition of the Euler angles $\Omega = (\alpha, \beta, \gamma)$ slightly altered as we just pointed out. Thus we may again expand $\sigma_\lambda(\Omega)$ in the basis set of $\varphi^L_{KM}(\alpha-\psi,\beta,\gamma)$. We will again obtain eq A7 but eq A8 will no longer generally be true, since Γ_Ω expressed in the (x^{iv}, y^{iv}, z^{iv}) coordinates will no longer be diagonal in this φ^L_{KM} basis set. (It is, of course, not even diagonal when expressed in the (x', y', z') coordinates if $R_{x'} \neq R_{y'}$.) However, the properties of the $\boldsymbol{M}$ and $(\boldsymbol{M}^2)^{(L,P)}$ are such that it can change only the K "quantum number" in operating on φ^L_{KM},[25,26,30,31] and these will correspond to different eigenvalues of $\Gamma_I\varphi^L_{KM}(\alpha-\psi,\beta,\gamma) = K^2R_I\varphi^L_{KM}(\alpha-\psi,\beta,\gamma)$. Since we are assuming $R_I >> R_x, R_y, R_z$, it then follows that these off-diagonal matrix elements will appear in second-order perturbation theory and may be neglected when the inequality is strong enough that first-order perturbation theory applies. Thus, to first order in R_x, R_y, R_z vs. R_I, one needs only the diagonal matrix elements, which may be obtained from the properties of Γ_Ω in eq A12 which are given elsewhere.[25,26,30,31] They are

$$\langle L_1K_1M_1|\Gamma_\Omega + \Gamma_I|L_1K_1M_1\rangle = \bar{R}L_1(L_1+1) + (1/2)(\bar{R} - R_{z^{iv}z^{iv}})(L_1[L_1+1] - 3K_1^2) + R_IK^2 \quad \text{(A14)}$$

where

$$\bar{R} \equiv \tfrac{1}{3}\,\mathrm{Tr}\,\mathbf{R} = \tfrac{1}{3}(R_{x'} + R_{y'} + R_{z'}) \quad \text{(A15a)}$$

while

$$(R_{z^{iv}z^{iv}} - \bar{R}) = -\frac{\sqrt{6}}{3}R^{iv(2,0)} \quad \text{(A15b)}$$

which may be expressed in terms of the $R^{(2,P)}$ principal components as

$$R^{iv(2,0)} = \sum_P \mathcal{D}^2_{0,-P}(\Theta^{-1})R^{(2,-P)} = \sum_P (-)^P \mathcal{D}^2_{+P,0}(\Theta)R^{(2,-P)} \quad \text{(A16)}$$

where $\mathcal{D}^2_{P,0}(\Theta) = \mathcal{D}^2_{P,0}(\alpha',\beta',\gamma') = \mathcal{D}^2_{P,0}(\alpha',\beta',0)$. [Thus we required the inverse transformation to that in eq A1.] Note that for axially symmetric rotational diffusion the angle α' in eq A16 is redundant, so it may be set equal to zero. Also note that by letting $({}^3/_2\bar{R} - {}^1/_2R_{z^{iv}z^{iv}}) \rightarrow R_\perp{}^{eff}$ and ${}^3/_2(R_{z^{iv}z^{iv}} - \bar{R}) \rightarrow R_\parallel{}^{eff}$, then the right-hand side of eq A14 becomes

$$R_\perp{}^{eff}L_1(L_1 + 1) + K_1{}^2(R_I + R_\parallel{}^{eff} - R_\perp{}^{eff}) \approx R_\perp{}^{eff}L_1(L_1 + 1) + R_IK_1{}^2 \quad \text{(A17)}$$

so by the previous discussions of cases 1 and 2 we see that the general case of anisotropic overall diffusion but with $R_I >> R_{x'},R_{y'},R_{z'}$ can be treated with the computer program based on the analysis of section II. One should also note that when the inequality $R_I >> R_{x'},R_{y'},R_{z'}$ no longer holds, the method outlined above (prior to the use of perturbation theory) allows one to obtain solutions of the general problem in terms of the basis set $\varphi^L_{KM}(\alpha-\psi,\beta,\gamma)$ instead of the more extended basis set $(1/(2\pi)^{1/2})e^{iK'\psi}\varphi^L_{KM}(\alpha,\beta,\gamma)$ used to obtain eq A3 and A4. However, one must treat the more complex diffusion operator of eq A12 in a coordinate frame in which it is not diagonal. Furthermore, this method does not appear to have any particular advantages for dealing with the problem of several internal modes of motion.

References and Notes

(1) R. P. Mason, C. F. Polnaszek, and J. H. Freed, *J. Phys. Chem.*, **78**, 1324 (1974).
(2) G. Rouser, G. J. Nelson, S. Fleisher, and G. Simon in "Biological Membranes, Physical Fact and Function", D. Chapman, Ed., Academic Press, New York, 1968, p 5.
(3) T. L. Steck and C. F. Fox in "Membrane Molecular Biology", C. F. Fox, Ed., Sinauer Associates, Stanford, Conn., p 27.
(4) D. Marsh, A. Watts, and P. F. Knowles, *Biochim. Biophys. Acta*, **467**, 109 (1977).
(5) L. Powers and N. A. Clark, *Proc. Natl. Acad. Sci. U.S.A.*, **72**, 840 (1975).
(6) L. Powers and P. S. Pershan, *Biophys. J.*, **20**, 137 (1977).
(7) L. Powers, Ph.D. Thesis, Harvard University, 1977.
(8) H. Gally, W. Niederberger, and J. Seelig, *Biochemistry*, **14**, 3647 (1975).
(9) S. J. Kohler and M. P. Klein, *Biochemistry*, **16**, 519 (1977).
(10) N. O. Petersen and S. I. Chan, *Biochemistry*, **16**, 2657 (1977).
(11) J. Seelig and H. U. Gally, *Biochemistry*, **15**, 5199 (1976).
(12) J. Seelig, H. U. Gally, and R. Wohlgermuth, *Biochim. Biophys. Acta*, **467**, 109 (1977).
(13) R. G. Griffin, L. Powers, J. Herzfeld, R. Haberborn, and P. S. Pershan, "Head Group Conformation in Phospholipids: A ^{31}P NMR Study of Oriented DPL Bilayers", XIXth Congress Ampere, Heidelberg, 1976.
(14) G. Büldt, H. U. Gally, A. Seelig, and J. Seelig, *Nature (London)*, **271**, 182 (1978).
(15) R. G. Griffin, *J. Am. Chem. Soc.*, **98**, 851 (1976).
(16) J. H. Freed and G. K. Fraenkel, *J. Chem. Phys.*, **39**, 326 (1963).
(17) J. H. Freed, G. V. Bruno, and C. F. Polnaszek, *J. Phys. Chem.*, **75**, 3385 (1971), referred to as FBP.
(18) S. A. Goldman, G. V. Bruno, C. F. Polnaszek, and J. H. Freed, *J. Chem. Phys.*, **56**, 716 (1972).
(19) J. H. Freed, "Spin Labeling: Theory and Applications", L. Berliner, Ed., Academic Press, New York, 1976, Chapter 3.
(20) G. V. Bruno, Ph.D. Thesis, Cornell University, Ithaca, N.Y., 1973.
(21) C. F. Polnaszek, G. V. Bruno, and J. H. Freed, *J. Chem. Phys.*, **58**, 3185 (1973).
(22) C. F. Polnaszek, Ph.D. Thesis, Cornell University, 1975.
(23) R. A. Haberkorn, J. Herzfeld, and R. G. Griffin, *J. Am. Chem. Soc.*, **100**, 1296 (1978).
(24) C. F. Polnaszek, S. Schreier, K. W. Butler, and I. C. P. Smith, submitted for publication in *J. Am. Chem. Soc.*
(25) A. R. Edmonds, "Angular Momentum in Quantum Mechanics", Princeton University Press, 1957.
(26) J. H. Freed in "Electron-Spin Relaxation in Liquids", L. T. Muus and P. W. Atkins, Eds. Plenum Press, New York, 1972, Chapter VIII.
(27) The Ivanov jump model [*Sov. Phys.—Usp.* (*Engl. Transl.*), **16**, 1 (1973)] is easily applied to internal rotations. In the strong-jump limit, the eigenvalues become $\tau_1^{-1}[1 - \delta_{K',0}]$, while intermediate-jump models have eigenvalues $R_1K'^2[1 + R_1\tau_1K'^2]^{-1}$, where τ_1 is the mean time between jumps, and $R_1\tau_1$ is proportional to the size of a mean diffusive step. (The inclusion of potential barriers to the internal motion is also straightforward by analogy with the full rotational problem (cf. ref 21).)
(28) S. Alexander, A. Baram, and Z. Luz, *Mol. Phys.*, **27**, 441 (1974), discuss another type of jump motion.
(29) This method can readily be generalized to the case where the magnetic nucleus is on an end group which is coupled to the main molecular framework via several single bonds, if we assume independent internal rotation about each bond. Thus for the case of two successive single bonds we can rewrite eq A1 as $F^{(L,K)}_{\mu,i} = \sum_{K',K'',K'''} \mathcal{D}^L_{KK'}(\Theta)\mathcal{D}^L_{K'K''}(\Psi_2)\mathcal{D}^L_{K''K'}(\Psi_1)F''^{(L,K''')}_{\mu,i}$, where $\Psi_1 = (\psi_1, \theta_1, \varphi_1)$, and $\Psi_2 = (\psi_2, \theta_2, \varphi_2)$, where ψ_1 and ψ_2 are the two angles of rotation, etc. Then one must use the diffusion operator $\Gamma_\Omega + \Gamma_{\Psi_1} + \Gamma_{\Psi_2}$ and expand in the basis set $(1/(2\pi)^{1/2})\varphi^L_{KM}(\Omega)e^{iK_1\psi_1}e^{iK_2\psi_2}$ to obtain the analogues of eq A3 and A4. For the simplified model of case 3, one then sets $K' = K'' = 0$ in the above expression for $F^{(L,K)}_{\mu,i}$.
(30) L. D. Favro, "Fluctuation Phenomena in Solids", R. E. Burgess, Ed., Academic Press, New York, p 79.
(31) W.-J. Lin and J. H. Freed, *J. Phys. Chem.*, in press.

Paramagnetic Oxides of Nitrogen Observed in a Sulfur Hexafluoride Matrix[1]

J. R. Morton, K. F. Preston,* and S. J. Strach[2]

Division of Chemistry, National Research Council of Canada, Ottawa, Ontario, Canada K1A OR9

(Received August 28, 1978) Publication costs assisted by the National Research Council of Canada

γ irradiation of a solid solution of nitrogen dioxide in sulfur hexafluoride generates a number of paramagnetic nitrogen oxides which exhibit isotropic EPR spectra at 110 K. The radicals NO_2, NO_3, and F_2NO have been positively identified, and a fourth species, hitherto unknown, is believed to be a radical ion of nitrosyl nitrate, $ONONO_2^{\pm}$.

Introduction

Historically, the oxides of nitrogen have provided an invaluable testing ground for the theories of chemical physics. Their presence in our atmosphere and the diversity of reactions which they undergo have ensured the lasting attention of kineticists; the interpretation of their spectra, particularly those of the paramagnetic oxides, has been a constant challenge to spectroscopists. All of the neutral odd-electron species, NO, NO_2, and NO_3, have been observed by EPR spectroscopy, but the detection and

0022-3654/79/2083-0533$01.00/0